Metabolic Engineering 60 (2020) 97–109

Contents lists available at ScienceDirect

Metabolic Engineering

journal homepage: www.elsevier.com/locate/meteng

Original Research Article

Improved biotin, thiamine, and lipoic acid biosynthesis by engineering the global regulator IscR

Anne P. Bali[a,b], David Lennox-Hvenekilde[a,b], Nils Myling-Petersen[b], Josi Buerger[b], Bo Salomonsen[b], Luisa S. Gronenberg[b], Morten O.A. Sommer[a], Hans J. Genee[b,*]

[a] The Novo Nordisk Foundation Center for Biosustainability, Technical University of Denmark, 2800, Kgs. Lyngby, Denmark
[b] Biosyntia ApS, Fruebjergvej 3, Copenhagen E, 2100, Denmark

ARTICLE INFO

Keywords:
Biotin
Lipoic acid
Thiamine
Vitamins
Iron-sulfur cluster
IscR

ABSTRACT

Biotin, thiamine, and lipoic acid are industrially important molecules naturally synthesized by microorganisms via biosynthetic pathways requiring iron-sulfur (FeS) clusters. Current production is exclusively by chemistry because pathway complexity hinders development of fermentation processes. For biotin, the main bottleneck is biotin synthase, BioB, a S-adenosyl methionine-dependent radical enzyme that converts dethiobiotin (DTB) to biotin. BioB overexpression is toxic, though the mechanism remains unclear. We identified single mutations in the global regulator IscR that substantially improve cellular tolerance to BioB overexpression, increasing *Escherichia coli* DTB-to-biotin biocatalysis by more than 2.2-fold. Based on proteomics and targeted overexpression of FeS-cluster biosynthesis genes, FeS-cluster depletion is the main reason for toxicity. We demonstrate that IscR mutations significantly affect cell viability and improve cell factories for *de novo* biosynthesis of thiamine by 1.3-fold and lipoic acid by 1.8-fold. We illuminate a novel engineering target for enhancing biosynthesis of complex FeS-cluster-dependent molecules, paving the way for industrial fermentation processes.

1. Introduction

Vitamins are organic compounds essential for both humans and animals. They are widely used in food, feed, cosmetics, and pharmaceuticals. Most vitamins are currently produced by chemical synthesis because of challenges in establishing economically competitive, biobased production alternatives. For some vitamins, including thiamine (vitamin B1), lipoic acid, and biotin (vitamin B7), slow catalysis of key enzymes is a significant barrier (Acevedo-Rocha et al., 2019; Cramer and Jarrett, 2018; Cronan, 2014; Palmer and Downs, 2013). The slow biosynthetic enzymes are phosphomethylpyrimidine synthase (ThiC) for the thiamine pathway, lysosomal acid lipase/cholesteryl ester hydrolase (LipA) for lipoic acid, and biotin synthase (BioB) for biotin. All are *S*-adenosyl methionine (SAM) radical enzymes that use iron-sulfur (FeS)-clusters for catalysis. These FeS-clusters are oxygen sensitive and require anaerobic conditions for isolation and *in vitro* studies, making the enzymes challenging to investigate (Broderick et al., 2014).

Production of some vitamins, such as riboflavin, has successfully transitioned from chemical synthesis to a biotechnology-based process, with others in development (Acevedo-Rocha et al., 2019; Schwechheimer et al., 2016). However, despite decades of strain engineering efforts by industry and academia (Brown et al., 1991; Sakurai et al., 1993; Xiao et al., 2019), commercial biobased production of biotin, thiamine and lipoic acid is too inefficient to replace the chemical synthesis processes (Brown and Komagowa, 1991).

A major bottleneck in biotin production is BioB, which catalyzes the last step in the pathway, converting dethiobiotin (DTB) to biotin (Fig. 1a) (Ifuku et al., 1995; Xiao et al., 2019). Evidence for the bottleneck is that engineered biotin cell factories accumulate DTB. An engineered *Bacillus subtilis* strain overexpressing native biotin genes reportedly produces 4 mg/L biotin and > 600 mg/L DTB in a 30 h fermentation, supplemented with 1 g/L pimelic acid and 7.5 g/L lysine (Van Arsdell et al., 2005). Xiao *et al.* also reports BioB as a bottleneck in *Pseudomonas mutabilis* cell factories producing 270 mg/L biotin in a fed-batch fermentation of 174 h supplemented with 1 g/L pimelic acid (Xiao et al., 2019). The highest reported fermentation titer of biotin is 600 mg/L, achieved by multiple rounds of random mutagenesis and antimetabolite selection combined with overexpression of a mutated biotin operon in *Serratia marcescens* (Masuda et al., 1995). However, also this strain accumulated DTB (200 mg/L) and fermentation time was 11 days, which is infeasible for industrial purposes. Despite these reports of progress, an additional 10–20 fold process performance is

* Corresponding author.
E-mail address: hjg@biosyntia.com (H.J. Genee).

https://doi.org/10.1016/j.ymben.2020.03.005
Received 18 December 2019; Received in revised form 24 February 2020; Accepted 12 March 2020
Available online 25 March 2020

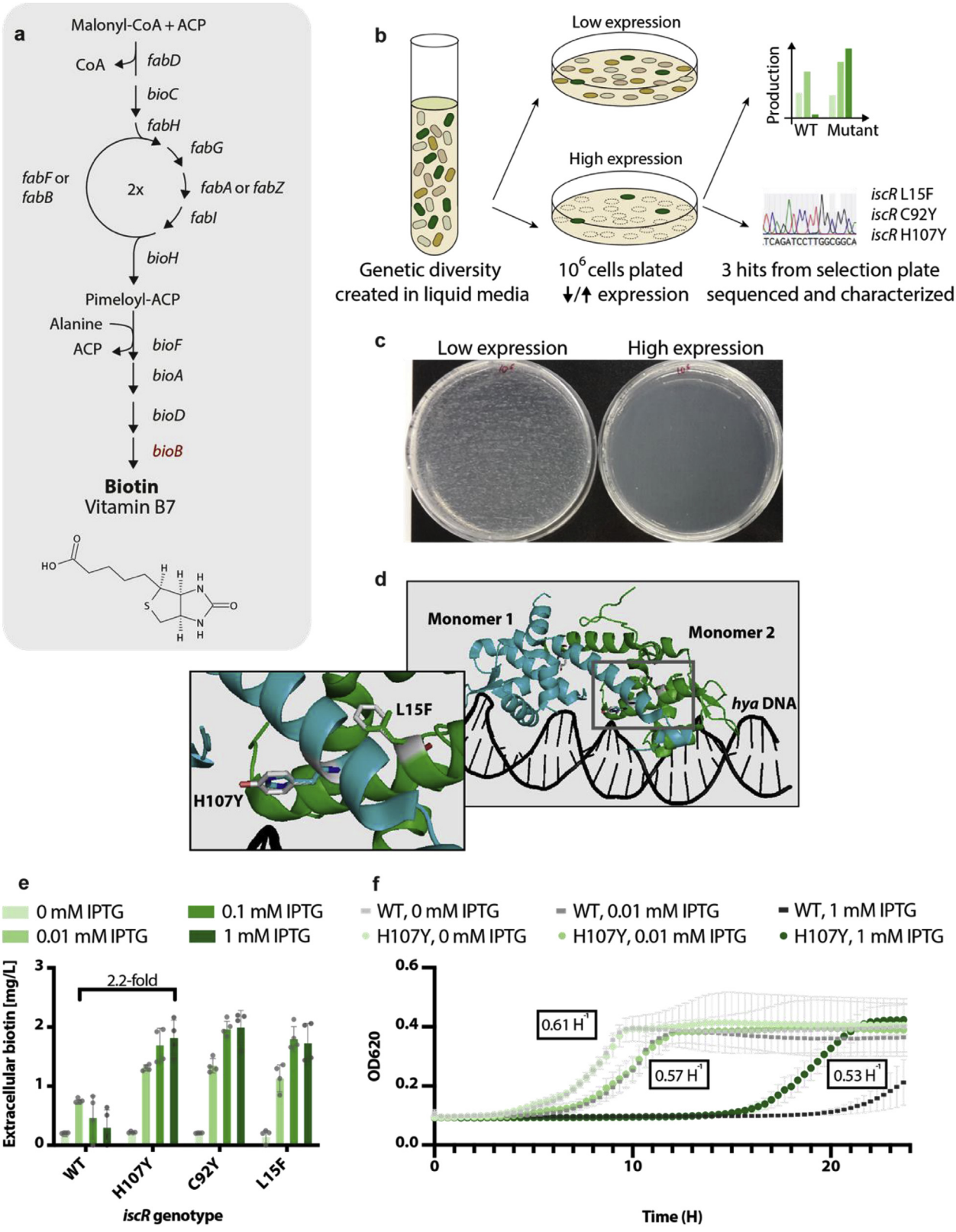

(caption on next page)

still required for an industrially competitive fermentation process.

The complex catalysis of BioB requires two SAM equivalents and sulfur donation from the [2Fe2S] cluster, one of two BioB FeS-clusters. This mechanism presumably requires cluster regeneration after each turnover (Cramer and Jarrett, 2018). BioB has a low turnover number and a slow catalysis when characterized *in vitro* (Broderick et al., 2014; Jarrett, 2005). In addition, when overexpressed *in vivo*, BioB inhibits growth (Ifuku et al., 1995), impeding development of biotin cell factories (Qiu et al., 2019; Sakurai et al., 1995). Ifuku *et al.* further demonstrated that growth inhibition by BioB overexpression is

Fig. 1. Mutant IscR increases tolerance to BioB expression and enables higher biotin production titers.
Toxicity when overexpressing BioB was used as the foundation for assays to select for colonies with improved tolerance for BioB expression. **a)** Schematic presentation of the *Escherichia coli* biotin biosynthesis pathway utilizing the fatty acid cycle for two rounds (2x) to build pimeloyl-ACP. The *bioB* gene encoding the FeS-cluster enzyme BioB is shown in red and important co-factors in gray. Abbreviations: SAM, *S*-adenosyl methionine, SAH, *S*-adenosylhomocysteine, AMTOB, *S*-adenosyl-2-oxo-4-methylthiobutyric acid, 5'-DOA, 5'-deoxyadenosine. **b)** General workflow for selecting mutant strains with increased BioB tolerance. **c)** Selection behavior on mMOPS plates of strains under low and high BioB expression: 10^6 cells were plated and incubated at 37°C for 24 h. **d)** Structural representation of dimerized apo-IscR bound to *hya* DNA with identified mutations in gray in stick drawings (L15F and H107Y; C92Y was not part of the crystal structure). **e)** Biotin production titers of three different IscR mutants identified through selection for improved tolerance to BioB expression. N = 4, error bars represent standard deviation. Individual replicates are shown in light gray circles. **f)** Growth rate data on IscR mutant strain H107Y at different induction levels, explicitly stated in black boxes. Darker color means increasing induction. N = 4, error bars represent standard deviation. (For interpretation of the references to color in this figure legend, the reader is referred to the Web version of this article.)

independent of the biotin-forming activity (Ifuku et al., 1995).

Multiple hypotheses exist for the observed toxicity of BioB overexpression including generation of reactive oxygen species (ROS) (Imlay, 2006; Van Arsdell et al., 2005), insufficient FeS-cluster supply or limitations in iron availability (Reyda et al., 2008), depletion of SAM/sulfur availability, and product inhibition by 5'-deoxyadenosine (Choi-Rhee and Cronan, 2005; Parveen and Cornell, 2011; Streit and Entcheva, 2003). The mechanisms of BioB overexpression toxicity are thus numerous and previous rational engineering strategies have had a low success rate.

Using growth selection, we identified specific point mutations that improve cellular tolerance to BioB overexpression and significantly increase biotin biosynthesis. All mutations were in a global regulator involved in FeS-cluster biogenesis. Using proteomics and various engineering strategies we elucidated main cellular effects caused by the mutations. We further show that the mutations improve lipoic acid and thiamine production titers. These results emphasize how synergistic effects might drive metabolic engineering efforts.

2. Results

2.1. Mutant IscR improves biotin cell factories

We exploited the toxic phenotype to select for mutant *E. coli* with increased tolerance for BioB overexpression (Fig. 1b). We built an expression construct that allowed BioB expression to be induced with isopropyl-β-D-thiogalactoside (IPTG) to levels that inhibit wildtype growth. At high BioB induction we observed a survival rate of approximately 1 in 10^6 plated cells (Fig. 1c). In order to generate diversity cells were passaged in liquid culture without any selection conditions. The resulting culture was then plated at the selective condition of high BioB induction. We had separately performed the selection in liquid medium, but found the final population to be less diverse as single fast-growing mutants quickly overtook the culture. Therefore we continued with selection on solid agar, choosing 90 surviving colonies from a population of $5{\cdot}10^6$ cells for further investigation, including confirmation of the improved growth phenotype as well as their DTB to biotin conversion rate. We hypothesized that some of these colonies might have spontaneous mutations that enabled them to tolerate higher levels of BioB expression. Five colonies that had improved biotin production levels were whole genome sequenced and their assembled genomes were compared to the parent. The sequencing revealed three unique strains that each harbored a single, unique mutation in the same gene: *iscR*, which encodes a dual regulator of *E. coli* FeS-cluster assembly. The three identified point mutations encode amino acid changes in *E. coli* IscR of L15F, C92Y and H107Y (Fig. 1d).

Strains with a mutant IscR were compared to the parent strain (BS1011) and evaluated as potential cell factories based on DTB to biotin conversion and growth profiles at several levels of induced BioB expression. Biotin formation profiles were similar for the three mutants (Fig. 1e), reaching maximum titers of almost 2 mg/L in minimal media representing a 2.2-fold increase in production over the parent strain. With a final OD600 of 2, this corresponds to a productivity of 0.1 mg/gCDW/h. Biotin production increased with IPTG induction of BioB expression from 0 to 0.1 mM IPTG, after which biotin titers plateaued at ~2 mg/L for the mutant strains. Production of the parent strain, however, started decreasing above 0.1 mM IPTG induction, correlating with significantly reduced growth (Fig. 1f). The three mutant strains had similar growth profiles (Fig. 1f has IscR H107Y only with data on other strains in Supplementary Fig. S3).

IscR is a global regulator in *E. coli*, affecting expression of more than 40 genes (Giel et al., 2006). IscR regulates FeS-cluster assembly through transcriptional repression of the *isc*-operon and activation of the *suf*-operon, which are the two main FeS-cluster biosynthesis pathways in *E. coli*. IscR activity depends on the intracellular FeS-cluster level, through IscR binding to a [2Fe2S] cluster (Fig. 2a, b). For example, IscR will only repress transcription of the *isc*-operon when bound to a [2Fe2S]-cluster (holo-form), while activation of the *suf*-operon by IscR may happen both in holo- and apo-form (without a [2Fe2S]-cluster) (Py and Barras, 2010). Four amino acids coordinate FeS-cluster binding in IscR: C92, C98, C104, and H107 (Fleischhacker et al., 2012). Two of the three mutated amino acids in the selected strains were part of this binding motif (C92Y and H107Y). The L15F mutation has not yet been described in the literature to our knowledge.

2.2. Proteomics elucidate cellular effects of IscR mutations

Having confirmed that the three strains with IscR mutations produced similar high titers of biotin, we elucidated the global protein changes caused by overexpressing BioB and mutating IscR. Nontargeted label-free proteomics quantification was carried out for mutant strain BS1353 (IscR H107Y) at two BioB induction levels (MutL, 0.025 mM IPTG induction, and MutH, 1 mM IPTG induction). Control strains were IscR wildtype (BS1011, WT) with the BioB expression plasmid and reference strain (BS1013, Ref) with native BioB expression, both at similar induction levels as the lowly induced BS1353.

Based on ANOVA analysis with Bonferroni correction for multiple testing, almost 200 proteins were differentially expressed in the mutant strain compared to a nonmutant IscR strain with wildtype BioB expression (Supplementary Table S4). Proteomics data showed that BioB protein levels were low in the wildtype strain without the BioB expression plasmid (~0% of total soluble protein, Ref). BioB levels were high in the wildtype strain with BioB overexpression induced at 0.025 mM IPTG (~1% of total soluble protein, WT). At 0.025 mM IPTG, the strain carrying the IscR mutation (MutL) had BioB levels similar to the wildtype, while at high induction (1 mM IPTG, which is toxic to wildtype cells), BioB levels were 2-fold higher than wildtype (~2% of total soluble protein, MutH). We further measured biotin production by the same four cultures after feeding with DTB and found that biotin levels correlated linearly with the level of soluble BioB (Fig. 2c). Hence, the data showed that the IscR mutation allowed cells to have higher levels of BioB protein and that BioB enzyme activity per protein was constant across induction levels and strain backgrounds.

Next, we considered the FeS-cluster biosynthesis pathways: The protein levels of most proteins from the *isc*- and *suf*-operons increased in the IscR mutant strain compared to the corresponding wildtype strain with BioB overexpression at induction with 0.025 mM IPTG. This result was consistent with the regulatory function of IscR. In the apo-form,

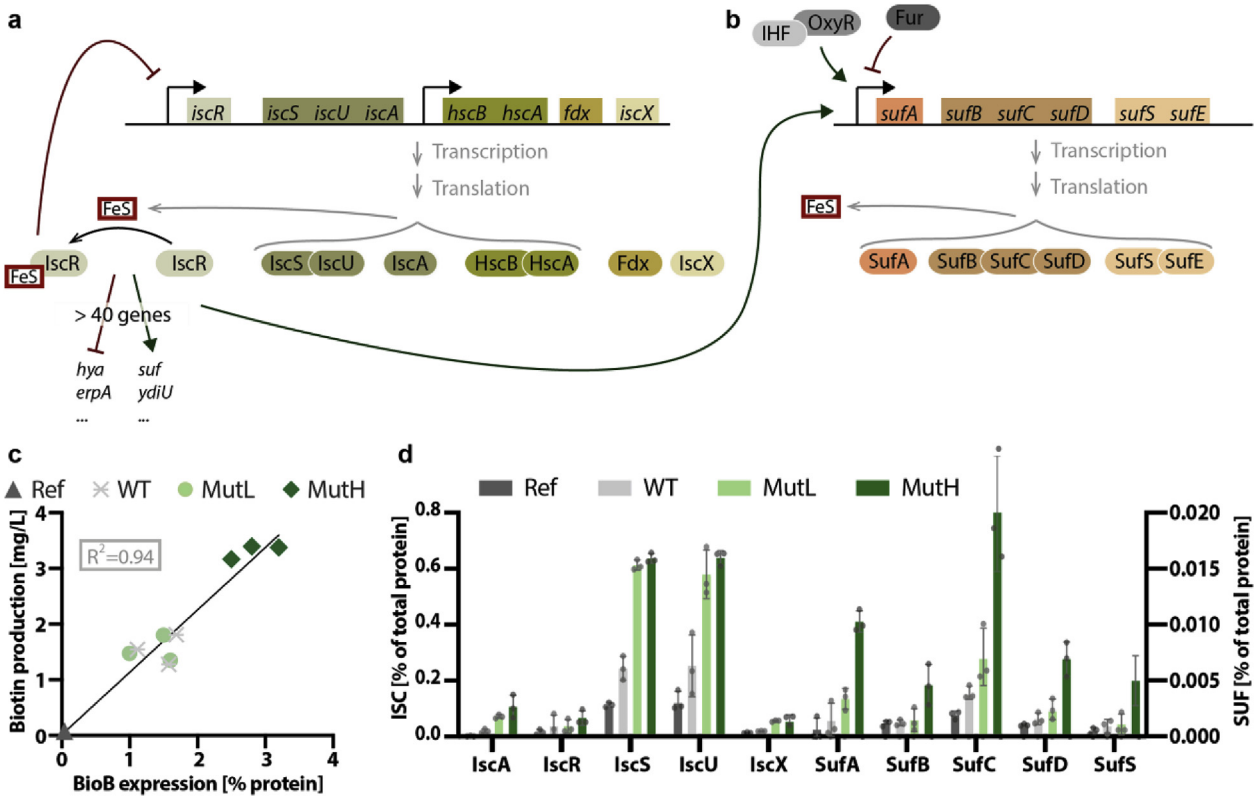

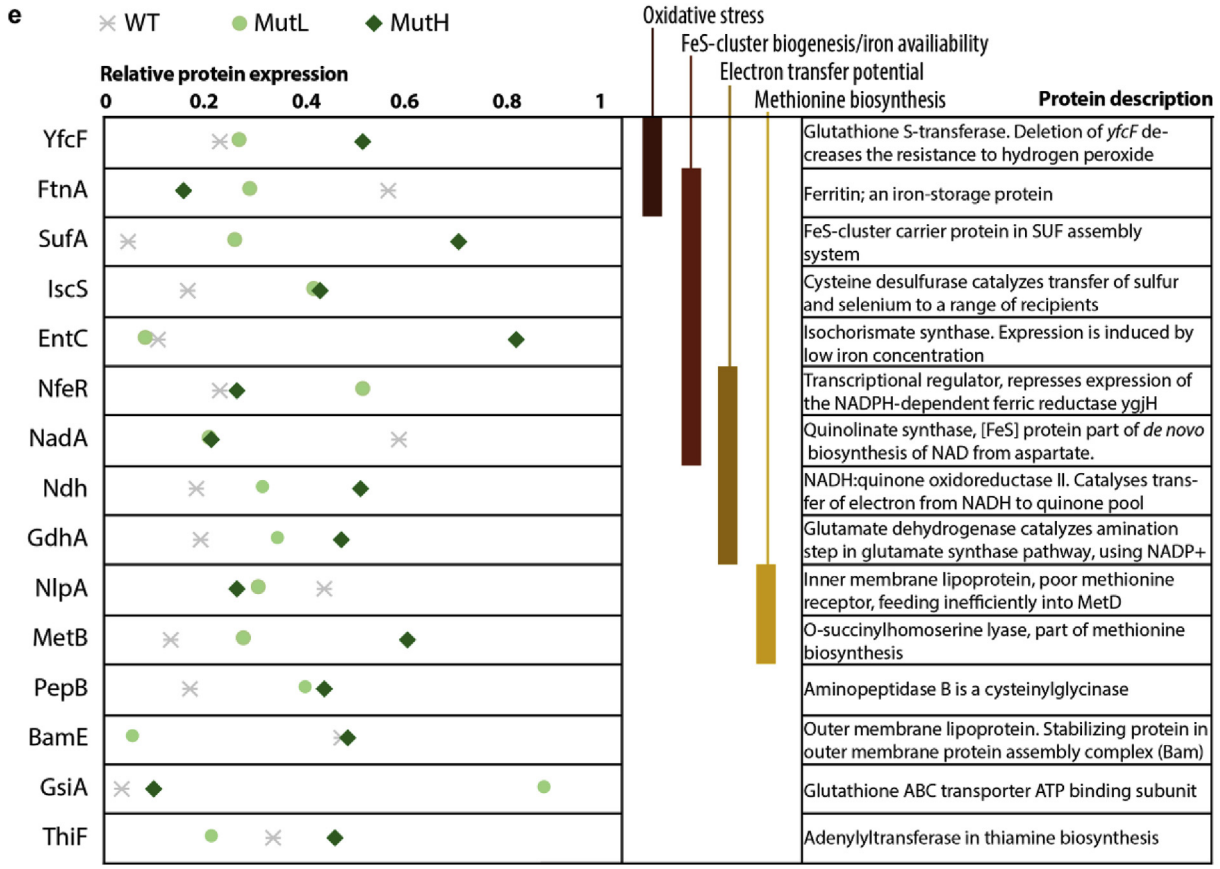

(caption on next page)

Fig. 2. Elucidation of the effects of identified IscR mutations using proteomics. *Isc*- and *suf*-operons constitute the two main pathways for FeS-cluster biogenesis, both regulated by IscR. Mutations in IscR were found in strains with elevated biotin production and proteomics was performed to compare protein levels in strains with and without IscR mutations. **a)** Schematic presentation of the *isc*-operon with the IscR regulatory mechanism. **b)** Schematic presentation of the *suf*-operon, including effects on expression from transcriptional regulators IHF, OxyR and FUR. **c)** Relationship between BioB protein expression and measured extracellular biotin produced from DTB for 3 strains at 2 induction conditions, low; 0.025 mM IPTG, high; 1 mM IPTG. Individual replicates are shown as separate dots, n = 3. **d)** Percentage protein content of proteins from *isc*- and *suf*-operons. N = 3, error bars represent standard deviation; individual replicates are in gray circles. **e)** Relative expression of proteins with significantly changed expression levels based on ANOVA with 95% confidence interval, Bonferroni correction, grouped based on protein function with potential influence on BioB reaction. Abbreviations in the figure; Ref: BS1013 (wildtype IscR) holding pBS430, induced at 0.025 mM IPTG, WT: BS1011 (wildtype IscR) holding pBS412, induced at 0.025 mM IPTG, MutL: BS1353 (IscR H107Y) holding pBS412, induced at 0.025 mM IPTG, MutH: BS1353 (IscR H107Y) holding pBS412, induced at 1mM IPTG.

without a bound FeS-cluster, IscR binds p_{sufA} to activate it and dissociates from p_{iscR} resulting in derepression (Fig. 2a, b) (Fleischhacker et al., 2012; Yeo et al., 2006). In the IscR mutant strain, levels of proteins from the *suf*-operon protein were even higher at high induction of BioB (1 mM IPTG) than at lower induction (0.025 mM IPTG) (Fig. 2d). The proteomics data suggested that toxicity observed in IscR wildtype cells overexpressing BioB could be due to FeS-cluster depletion.

To understand the global effects of mutating IscR, we used proteomics data to compare the relative protein levels of wildtype and mutant IscR strains with functional BioB expression plasmids: 15 proteins had significantly changed levels (Fig. 2e), of which only SufA, IscS and NfeR (YqjI) are members of the IscR regulon (Giel et al., 2006). Comparing protein levels of strains at low induction (0.025 mM IPTG, WT and MutL), we observed that SufA, IscS, NfeR, Ndh, GdhA, MetB, PepB, and GsiA levels were increased in the IscR mutant strain (MutL), while protein levels of FtnA, NadA, NlpA, BamE and ThiF were decreased. Similarly, we found that levels of SufA, Ndh, GdhA and MetB further increased and FtnA further decreased in IscR mutant strains with high BioB induction (MutH) compared to low BioB induction (MutL). Also, in IscR mutant strains, relative protein levels of YfcF, EntC, BamE and ThiF were higher with high BioB expression than low expression while NfeR and GsiA levels were lower.

We observed an effect on the level of proteins involved in oxidative stress, iron availability and electron transfer potential such as YfcF, EntC and Ndh (Kanai et al., 2006; Nahlik et al., 1989; Price and Driessen, 2010). Also, biosynthesis of methionine, a highly oxidation-sensitive amino acid (Ezraty et al., 2017), was affected by mutation in IscR through MetB and NlpA (Ferla et al., 2019; Zhang et al., 2003), which are involved in methionine biosynthesis, although the mechanism is not clear. These results illustrate that the effects of mutating IscR were global and likely extended beyond FeS-cluster biogenesis.

2.3. Combining IscR mutations was not additive

We hypothesized that the three identified IscR mutations each disrupted FeS-cluster binding. If binding was completely disrupted by each mutation, combining the mutations would have no synergistic effects. However, if binding was only partially disrupted, combining the mutations could lead to full FeS-cluster binding disruption, leading to the phenotypic effect of further increased biotin production. The effect of combinatorial mutations in IscR as well as *iscR* deletion on expression of enzymes in the *isc*- and *suf*-pathways, has been investigated in detail for other processes (Fleischhacker et al., 2012; Yeo et al., 2006). Substituting alanines for any or all of the three FeS-coordinating cysteines of IscR results in similar changes in expression from the *sufA* and *iscR* promoters (Yeo et al., 2006). A similar expression profile is seen in strains with an IscR H107A mutation (Fleischhacker et al., 2012). However, expression profiles from strains combining mutations in H107 with any FeS-cluster coordinating cysteines have not been reported.

We introduced the three mutations we identified in all seven combinatorial possibilities using multiplex genome engineering and tested for biotin production under expression conditions of 0, 0.01 and 0.1 mM IPTG (Fig. 3a). Overall, biotin production profiles for the combinatorial mutant strains were comparable to the single-mutant strains. This result suggested that mutating either of the FeS-cluster coordinating amino acids completely disrupted the IscR FeS-cluster binding ability. Also, mutant strains with the L15F substitution in IscR had a production profile similar to the other strains. From the IscR crystal structure, position L15 is proximal to the FeS-cluster coordinating amino acid H107Y (Fig. 1d). We do not further elucidate the structural mechanism of the L15F mutation. The phenotypic effect of this mutation is similar to the two mutations that disrupt binding of the FeS-cluster in IscR in all variables measured. Therefore, we expect the L15F mutation to also disrupt binding of the FeS-cluster to IscR.

2.4. Comparing engineering strategies for FeS-cluster supply

Our results indicated that FeS-cluster assembly was a limiting factor in BioB expression. We tested if previously reported engineering strategies to enhance FeS-cluster availability for other FeS-cluster enzymes through rational modification of *iscR* further improved BioB expression and biotin production. Deleting *iscR* to derepress the *isc*-operon has been shown to improve hydrogenase activity and hydrogen production in *E. coli* (Akhtar and Jones, 2008; Kuchenreuther et al., 2010). In addition to engineering IscR, overexpression of either the *isc*- or *suf*-operons improves expression and/or activity of the FeS-cluster enzymes holo-ferredoxins (Nakamura et al., 1999), nitrogenases (Li et al., 2016), LipA (Kriek et al., 2003) and IspH (Gräwert et al., 2007).

We generated an *iscR* knockout strain by introducing premature stop codons at amino acid positions 22 and 33 of *iscR* (Fig. 3b) and biotin production was evaluated at three induction conditions (0, 0.01, and 0.1 mM IPTG). The *iscR* knockout strains had production profiles comparable to the IscR wildtype strain and growth toxicity from BioB overexpression was not mitigated. Deleting *iscR* increases p_{iscR} expression and decreases p_{sufA} expression (Yeo et al., 2006). The finding that *iscR* knockout strains were similar to the IscR wildtype strain suggested that the expected increase in *isc*-operon expression did not supply enough FeS-cluster formation capacity to overcome growth inhibition from BioB overexpression.

The effect on biotin production from overexpressing the *isc*- and *suf*-operons was evaluated using plasmid libraries expressing native *E. coli sufABCDSE* or *iscSUA-hscBA-fdx-iscX* operons with 16 different constitutive promoters with predicted strength ranging from 3 arbitrary units (AU) to 866 AU (V K Mutalik et al., 2013). Cells with the libraries had low viability, with only four unique operon plasmids identified from 96 sequenced colonies. More than half of the sequenced colonies had lost the *isc*- or *suf*-plasmid, suggesting that plasmid expression was a burden to the cells. The strongest identified predicted promoter strength was 156 AU for the *isc*-operon and 99 AU for the *suf*-operon (Supplementary Table S2), which was at the lower end of the library range. We did not investigate if host viability correlated with promoter strength.

We evaluated the effect on biotin production of the four uniquely identified constructs (Fig. 3c). Co-expression of either the *isc*- or the *suf*-operon constructs with the BioB-overexpressing plasmid improved biotin titers 1.2-fold to 2-fold compared to the wildtype IscR control strain. The best-performing auxiliary construct expressed the *suf*-operon from the apFAB251 promoter with a predicted strength of 30.1 U (Vivek K Mutalik et al., 2013) and had approximately 80% the biotin production of the reference strain with mutated IscR (suf-D7 vs. IscR

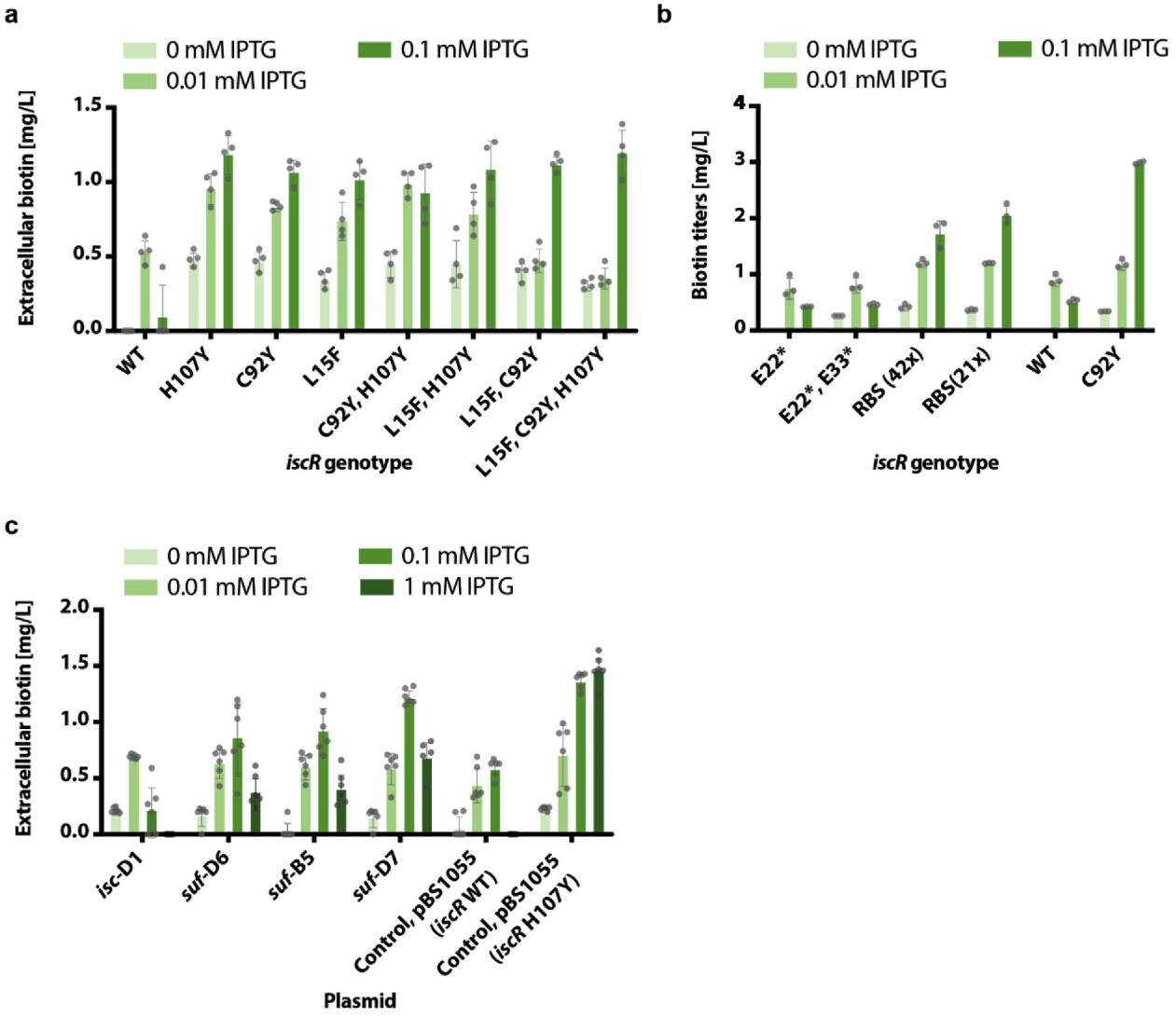

Fig. 3. FeS-cluster engineering in *E. coli*. After identifying three unique mutations in IscR, hypothesized to affect FeS-cluster binding, metabolic engineering strategies were used to evaluate and compare effects on biotin production. Error bars represent standard deviation and individual replicates are in gray circles. All strains expressed BioB from plasmid pBS412. **a)** Biotin production data for a combinatorial IscR mutant strain compared to a single mutant strain and wildtype reference strain (WT) (n = 4). Naming is based on IscR genotype. **b)** Biotin production data of *iscR* knockout strains (E22* +/− E33*) and strains with predicted increased expression of the C92Y IscR mutant through RBS, ribosome binding site, engineering. The predicted relative increases are 21x and 42x. Expression is compared to an IscR mutant strain with native RBS and IscR wildtype (n = 3). **c)** Biotin production data of IscR wildtype (WT) strains carrying plasmids expressing promoter libraries of *isc*- or *suf*. Mutant and wildtype IscR control strains carried control plasmid expressing GFP instead of *isc*- or *suf*-operon (n = 6).

H107Y, Fig. 3c).

Plasmid overexpression of *isc*- and *suf*-operon was hypothesized to be a burden to cells based on low viability with the expression library, which is a drawback for the genetic stability of cell factories (Rugbjerg et al., 2018). We hypothesized that a stronger ribosome-binding site (RBS) in front of mutant *iscR* would elevate levels of apo-IscR, leading to *suf*-operon activation and slightly higher *isc*-operon expression (Fig. 4), while being a lower burden to the cells compared to plasmid overexpression of *isc*- or *suf*-operon. However, engineering to increase RBS strength did not increase biotin titer. Mutant IscR strains with an altered RBS produced more biotin than the IscR wildtype strain but ~30% less than strains with native RBS (Fig. 3b). The decrease in biotin production could be due to predictions about RBS strength, which have high inaccuracy (Salis, 2011), or might be caused by altered expression in parts of the IscR regulon other than *isc* and *suf*.

2.5. IscR mutations improve production from other FeS-cluster-dependent pathways

We investigated if other potential cell factories with FeS-cluster enzymes benefited from IscR mutations. ThiC in thiamine biosynthesis and LipA in lipoic acid biosynthesis are FeS-cluster enzymes that are proposed bottlenecks in their production because of low catalytic rates (Cronan et al., 2005; Palmer and Downs, 2013). We hypothesized that, like BioB, increased expression of these enzymes would improve flux towards their products, but with a high risk of FeS-cluster depletion.

In the lipoic acid biosynthesis pathway (Fig. 5a), LipA catalyzes the last step converting octanoic acid to lipoic acid. Plasmid overexpression of the *isc*-operon improves expression of soluble LipA in cell lysates (Kriek et al., 2003). Based on Fe and S measurements in soluble vs. insoluble cell lysate fractions, Kriek *et al.* suggest this increase is due to increases in FeS-cluster-bound holo-LipA, with apo-LipA in the insoluble fraction. Catalysis by LipA is reported to be similar to BioB catalysis, requiring [4Fe4S] cluster regeneration for multiple turnovers

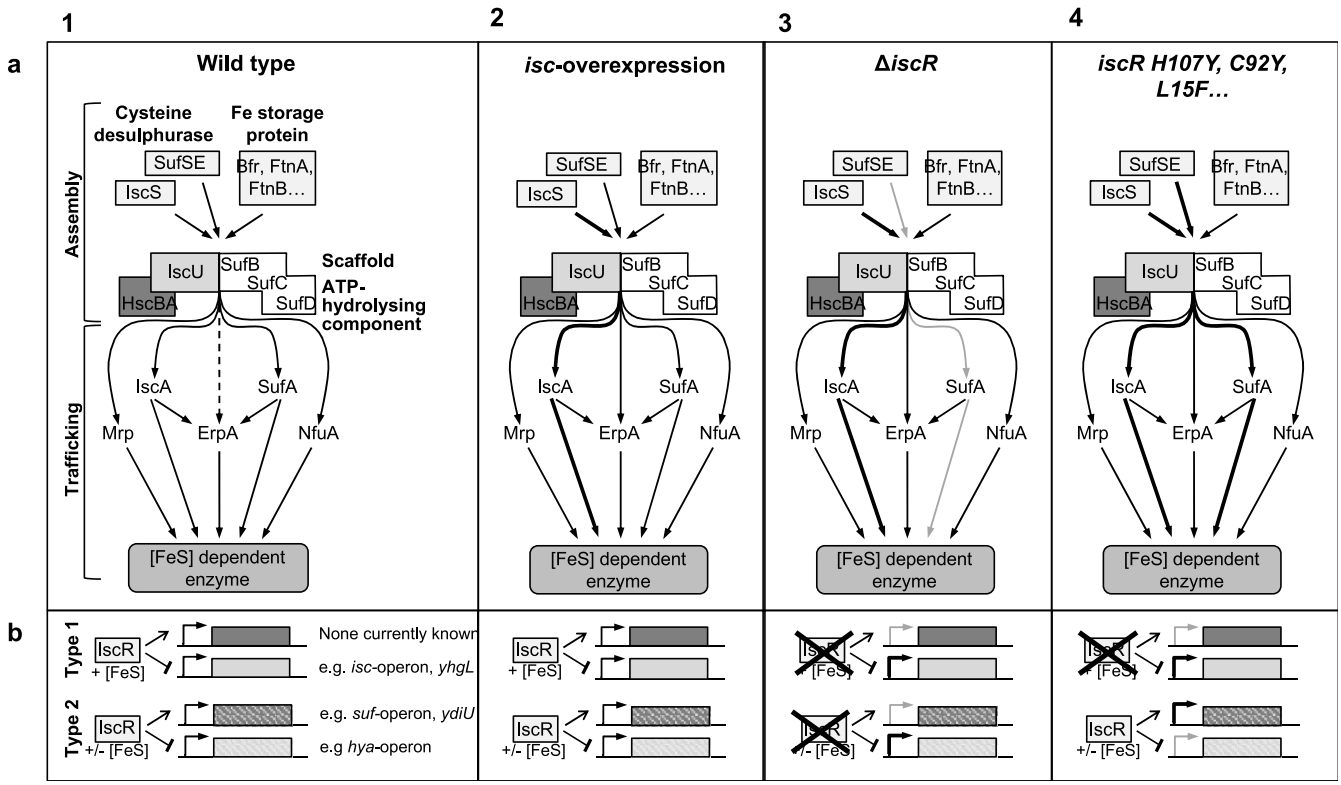

Fig. 4. Effect of Isc mutations on expression of FeS-cluster biogenesis genes and promoters regulated by IscR. a) 1, Overview of FeS-biogenesis pathway in wildtype *E. coli*; 2–4, expected relative expression changes in the pathway in indicated *isc*-mutant strains. **b)** 1, Expression from IscR-controlled Type 1 and Type 2 promoters in wildtype *E. coli*; 2–4, Expected relative expression in *isc*-mutant strains compared to wildtype. No data were available on IscR expression and relative abundance of holo-IscR and apo-IscR in the *isc*-overexpression strain, but expression of IscR (and the genomically encoded *isc*-operon) was likely downregulated due to increased FeS-cluster incorporation into IscR.

(Cronan, 2013; McCarthy and Booker, 2017). Due to these similarities, we hypothesized that the reaction catalyzed by LipA would also benefit from mutations in IscR. Cell factories for lipoic acid production were established similar to the biotin cell factories, expressing LipA from an inducible plasmid. Because lipoic acid is synthesized *in vivo* as covalently attached lipoylated lipoyl domains to specific enzymes (Cronan, 2013) (Fig. 5a), we co-expressed a truncated version of a lipoylated pyruvate dehydrogenase subunit encoded by *aceF* (Ali and Guest, 1990; Sun et al., 2017). Production of free lipoic acid was evaluated in strains with and without IscR mutations (C92Y and H107Y) after 24 h growth in minimal media supplemented with octanoic acid. Growth profiles for IscR C92Y and wildtype IscR were generated under different LipA induction levels (Fig. 5b). The mutant strain had higher LipA expression than the wildtype strain, alleviated overexpression toxicity, and improved production titers of extracellular, free lipoic acid (Fig. 5c). Even though most lipoic acid is expected to be protein bound, a small fraction is released as free lipoic acid by unidentified mechanisms. We assumed this level to correlate with the total amount of protein-bound lipoic acid generated. The mutant strains produced 9.3 μg/L free, extracellular lipoic acid when LipA expression was induced, representing a 1.8-fold increase compared to the wildtype IscR strain (Cronan et al., 2005).

Similar to lipoic acid, the effects of mutations in the FeS-cluster binding site of IscR were tested on thiamine production in bacterial cell factories. Thiamine has a complex biosynthetic pathway with two branches and seven core genes (Fig. 5d), of which two encode radical SAM enzymes (ThiC and ThiH) (Jurgenson et al., 2009). Improvements in chemical synthesis of thiamine (Eggersdorfer et al., 2012) have generated a highly efficient process. Cost-competitive microbial production will require extensive improvements (Acevedo-Rocha et al., 2019) but little metabolic engineering has been reported in the literature on the thiamine pathway (Schyns et al., 2005). A study using transposon mutants identified several genes related to FeS-cluster homeostasis that were affected in strains with altered thiamine production (Cardinale et al., 2017), supporting thiamine as a good fit for testing the IscR mutations. We established an *E. coli* thiamine cell factory by overexpressing the native *thiCEFSGH* operon on a plasmid with a strong constitutive promoter. Based on initial characterization, the thiamine production strain was limited by the SAM radical enzyme ThiC. Each identified mutation in the FeS-cluster binding site of IscR that was beneficial for BioB expression was introduced into the strain. Extracellular thiamine production evaluated after incubation for 24 h in minimal media showed a 1.3-fold increase in thiamine production by the mutant strains compared to the optimized parent cell factory, for a titer of 1.9 mg/L extracellular thiamine (Fig. 5e). This further represents a 1.5 fold improvement over the previously best reported titer of 1.3 mg/L based on engineered *Bacillus subtilis*(Schyns et al., 2005).

3. Discussion

Improving BioB has long been limiting for establishing high-producing biotin cell factories (Ifuku et al., 1995; Van Arsdell et al., 2005; Xiao et al., 2019). We demonstrate that single mutations in the IscR regulator diminish growth inhibition because of BioB overexpression and enable a 2.2-fold increase in biotin production compared to a strain expressing BioB to the limit of toxicity (Fig. 1e, f). Based on these results and previous reports that C92, C98, C104 and H107 in IscR are responsible for FeS-cluster binding (Fleischhacker et al., 2012; Yeo et al., 2006), we hypothesize that our mutant strains generate an IscR protein that is always in apo-IscR form regardless of cellular FeS-cluster concentration. FeS-cluster binding determines the regulatory nature of IscR, which has a central role in FeS-cluster biogenesis (Py and Barras, 2010). IscR in apo-form only, would constantly derepress the *isc*-operon

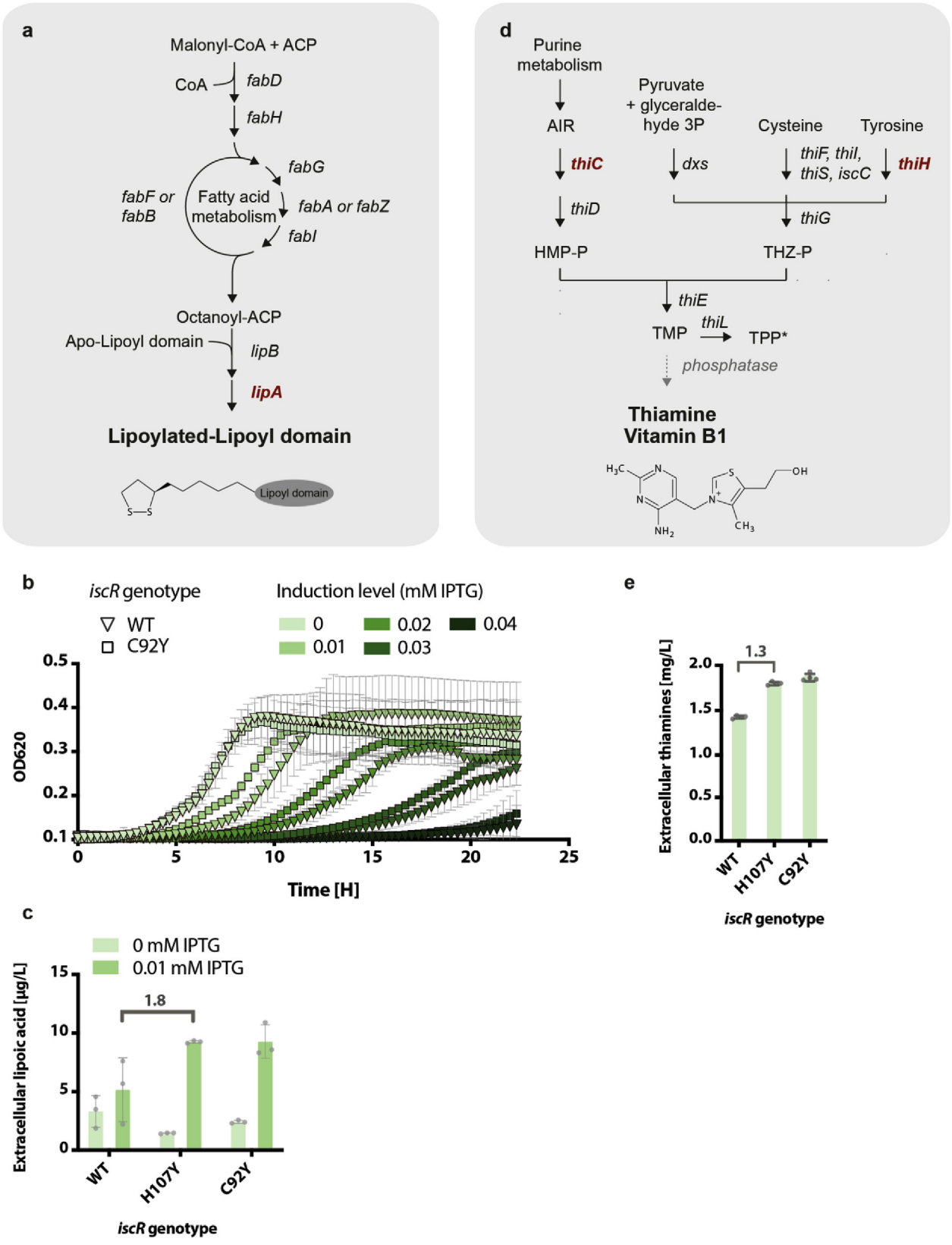

Fig. 5. Effects of IscR mutations on other biosynthetic pathways with FeS-cluster enzymes. a) Lipoic acid biosynthetic pathway in *E. coli*. **b)** Growth rate data on LipA-overexpressing strains with (squares) and without (triangles) mutation in IscR for five induction levels from 0 mM to 0.04 mM IPTG (darker green indicates increasing IPTG concentration) (n = 3, error bars represent standard deviation). **c)** Lipoic acid production titers of strains with and without mutation in IscR (n = 3, error bars represent standard deviation, individual replicates are in gray circles). **d)** Thiamine biosynthetic pathway in *E. coli*. **e)** Thiamine production titers of strains with and without mutation in IscR (n = 4, error bars represent standard deviation, individual replicates are in gray circles). Red, FeS-cluster enzymes. (For interpretation of the references to color in this figure legend, the reader is referred to the Web version of this article.)

and activate the *suf*-operon (Fleischhacker et al., 2012; Yeo et al., 2006), increasing FeS-cluster biogenesis (Fig. 2a,b,e, 4). Increased expression of Isc-proteins in *iscR* mutant strains confirms the observation from literature. The additional increase of Suf-proteins between IscR mutant strains with low (MutL) and high (MutH) induction of BioB (Fig. 2b) suggests a change in regulation from Fur and/or OxyR-IHF, potentially due to altered stress-conditions when increasing expression of BioB. The observation that upregulation of FeS-cluster biogenesis reduced growth toxicity from BioB overexpression suggested that FeS-cluster depletion is a main contributor to the observed toxicity in IscR wildtype strains. Insufficiencies in FeS-cluster formation can lead to inactivation of other, essential FeS-cluster proteins, including members of the TCA cycle such as those encoded by *acnA*, *acnB*, *fumA* and *fumB* (Py and Barras, 2010).

We evaluated overexpressing the *isc*- or *suf*-operon as an alternative way to improve FeS-cluster supply and affect biotin production. Plasmid-based overexpression of either the *suf*- or *isc*-operon improves catalysis of FeS-cluster enzymes such as nitrogenases (Li et al., 2016), LipA (Kriek et al., 2003) and IspH (Gräwert et al., 2007). Although biotin production improvements ranged from 1.2 to 2-fold (Fig. 3c) when overexpressing *isc*- and *suf*-operon at different levels, the strains holding the plasmid libraries had low viability. One possible explanation is that the plasmid that highly expressed entire operons was a higher burden to cells than genomically engineered improvements in FeS-cluster supply. Metabolic burdens and toxicities are major drawbacks for cell factory scale-up (Rugbjerg and Sommer, 2019) and even small differences in these can have a large impact on production stability over generations of growth in industrially relevant fermentation scales (Rugbjerg et al., 2018; Rugbjerg and Sommer, 2019). Single point modifications in genomic IscR seemed to burden cells less than plasmid overexpression of *isc*- and *suf*-operons and offer a more elegant solution with greater freedom to quickly test the effect of other plasmid-expressed genes that might benefit biotin production. In summary, the findings supported the hypothesis that FeS-cluster supply was a limiting factor in strains overexpressing BioB, because biotin production improved over wildtype IscR when FeS-cluster biogenesis was improved.

Our improved production strains reach 2 mg/L after 24 h of small-scale batch fermentations with a biotin productivity of 0.1 mg/gCDW/h. For comparison, the previously best reported biotin productivities are ~0.003 mg/gCDW/h for *B. subtilis*(Van Arsdell et al., 2005), ~0.02 mg/gCDW/h for *P. mutabilis*(Xiao et al., 2019) and ~0.04 mg/gCDW/h for *S. marcensens*(Masuda et al., 1995), indicating a 2.5-fold higher productivity for our strain over previous reported efforts. However, it should be kept in mind that the growth conditions compared are very different; 400 µl batch-cultures in minimal media vs. 2 L fed-batch fermentations in various complex growth media. Furthermore, the biomasses are estimates based on reported optical densities which may change with more precise values for cell mass.

BioB is suggested to be a “suicide enzyme” with one or fewer turnovers per monomer *in vitro* (Berkovitch et al., 2004; Jarrett, 2005). From our proteomic analysis, we observed that extracellular biotin levels correlated linearly with levels of measured BioB protein. These observations neither confirmed nor rejected the hypothesis of BioB as a true suicide enzyme. The catalytic [2Fe2S]-cluster (Cramer and Jarrett, 2018) may be regenerated during BioB catalysis, similar to one of the two [4Fe4S]-clusters in LipA. NfuA also efficiently reconstitutes the [4Fe4S] auxiliary cluster during LipA catalysis in a non-rate-limiting step (McCarthy and Booker, 2017). However, the factors responsible for a potentially similar mechanism in BioB remain to be identified.

When mutating a global regulator such as IscR, which has a regulon of more than 40 genes (Giel et al., 2006) including some that also have regulatory roles, several pathways are likely to be affected and rationally predicting all changes can be difficult. While limitations in FeS-cluster supply and repair are likely to be main factors explaining BioB toxicity, based on the direct effect of mutating IscR on *isc*- and *suf*-operon expression (Fig. 2d), proteomics suggested that other areas might also be affected. These areas include oxidative stress tolerance, iron availability, methionine biosynthesis and redox potential (Fig. 2e). Metalloproteins such as FeS-cluster enzymes are prone to damage by ROS leading to oxidative stress (Imlay, 2006). The decrease in FtnA protein levels in the IscR mutant strain compared to the wildtype strain at low BioB induction (Fig. 2e) could be an effect of improved expression of FeS-cluster biogenesis proteins resulting from mutating IscR (Yeo et al., 2006). FtnA is a ferritin used to store iron or damaged FeS-clusters to avoid ROS generation (Bitoun et al., 2008). An increased ability to synthesize and repair FeS-clusters would decrease the need for scavenging. In addition to improving FeS-cluster generation, IscR mutations in the FeS-cluster binding site are reported in *E. coli* strains evolved for increased tolerance of oxidative stress using treatment with paraquat (Yang et al., 2019). Yang *et al.* explain the increased tolerance to oxidative stress as increased FeS-cluster biosynthesis to overcome predicted mismetallation of IscU, the FeS-cluster assembly protein of the *isc*-pathway (Yang et al., 2019). These observations are consistent with our finding that mutations in IscR affects both FeS-cluster shortage and cellular oxidative stress levels, helping to mitigate the growth inhibition from BioB overexpression. Additional omics analyses such as transcriptomics and metabolomics could further elucidate the cellular effects of mutating IscR and assist in expanding the explanation for BioB toxicity.

Finally, we demonstrated improvements of 1.8-fold for lipoic acid titers and 1.3-fold for thiamine production (Fig. 5) by introducing the IscR mutations into lipoic acid and thiamine production strains. Since the biosynthesis of lipoic acid and thiamine both depend on FeS-cluster enzymes for key enzymatic steps (Cronan et al., 2005; Palmer and Downs, 2013), the improvement in titers confirmed that the FeS-cluster (s) in BioB are the most likely source of growth inhibition when BioB is overexpressed. The results further emphasize the likelihood of increased FeS-cluster supply and repair as the main reason for improvements in strains with mutated IscR.

The induction levels of *lipA* required to reach toxicity are approximately 10- to 100-fold lower than for *bioB* (Fig. 1e). We cannot expect that the protein levels for BioB correspond to the protein levels of LipA at the same induction levels due to expected differences in translational initiation rate, mRNA stability, protein stability etc. Therefore, we cannot know if the toxicity of LipA is caused by the same factors as for BioB. However, what is evident from the data is, that the IscR mutation does reduce the toxicity, as is the case for BioB, which indicates that FeS-cluster draining is part of the LipA toxicity.

The finding that three independent biosynthesis pathways had improved production titers indicated that the mutations in IscR likely disrupted its regulatory FeS-cluster binding and have broad platform potential. Mutating the FeS-cluster binding site of IscR will likely benefit other cell factories with FeS-cluster enzymes. The results show how the consequences from such mutations can benefit production of different compounds when the mutations are involved in a metabolic hub branching to many different metabolites. Our findings emphasize how tools to improve production of some compounds and their synergistic effects may accelerate the development of cell factories for high-value compounds. Mutating the FeS-cluster binding site of IscR is likely to benefit additional FeS-cluster enzymes.

4. Methods

4.1. Materials and media

All chemicals were from Sigma Aldrich or Carl Roth unless otherwise stated. Minimal MOPS media was made as described in Supplementary Note 1 and used as standard assay medium unless otherwise stated. Minimal MOPS succinate media was prepared as minimal MOPS media, replacing glucose with 50 mM succinic acid disodium (final concentration). Biotin stock solution was prepared in DMSO to a final concentration of 100 mM and then diluted in mMOPS.

Lipoic acid stock solution was prepared in ethanol to a concentration of 1 g/L with dilutions made in minimal MOPS succinate medium. Plasmid and PCR purifications were performed according to manufacturers' guidelines, using E.Z.N.A. Plasmid Mini Kit I, V-spin and E.Z.N.A. Cycle Pure Kit I from VWR.

4.2. Isolating iscR mutant strains

The biotin selection system was based on a single plasmid encoding an IPTG-inducible *E. coli bioB* gene combined with a biotin auxotrophic BW25113 Δ*bioB* strain. Cell cultures grown for several generations and passaged for 4 days were plated on mMOPS plates with kanamycin (50 μg/mL) and 0.1 mM IPTG to induce BioB expression to toxicity. Cells appearing on induction plates after 24 h incubation at 37 °C were characterized as described in the main text. In-depth characterization of the selection system is in Supplementary Note 2.

4.3. Strains and plasmids

See Supplementary tables S1-S3.

4.4. Structural investigations of IscR mutants

The identified IscR mutations were highlighted by "stick drawings" in the protein structure of apo-IscR bound to *hya* DNA (PDB ID: 4HF1 (Rajagopalan et al., 2013)) using PyMOL v. 1.7 (Delano W. L., 2002). Each mutated amino acid was changed from the original by copying the residue followed by the "Wizard Mutagenesis" tool. Changing the visualization to stick drawings were done using "sticks" under "show" options.

4.5. Construction of modified IscR strains

Combinatorial IscR mutant strains, *iscR* knockout and RBS mutant-*iscR* strains were constructed using up to 6 rounds of MAGE (Wang and Church, 2011). Briefly, BS1011 holding pBS136 was grown in 4 mL Luria broth (LB) with 100 μg/mL ampicillin at 37°C with shaking (250 rpm) in culture tubes. At OD600 0.5, 400 μl 20% arabinose was added to induce the λ-Red system. Incubation continued for 30 min, after which cells were placed on ice for 5 min, spun down in a precooled centrifuge at 5000G for 5 min and washed twice in 2 mL icecold water. Cells were collected by centrifuging at 5000G for 5 min and resuspended in 200 μl icecold water. A 45-μl cell suspension was transferred to precooled 1 mm electroporation cuvette and mixed with 5 μl 100 μM oligo stock (or oligo pool) followed by electroporation at 1800 V before 950 μl prewarmed SOC media were quickly added and cells transferred to growth tubes for incubation for 1–2 h. Three mL LB with 100 μg/mL ampicillin was added, and procedures repeated up to 6 times to OD600 0.5. Successful introduction of mutations was evaluated by colony PCR using oBS1670 and oBS1991, annealing temperature 56°C, and elongation time 2 min with subsequent sequencing of purified PCR constructs. MAGE oligos were designed using MODEST software (Bonde et al., 2014) (Supplementary Table S3).

4.6. Construction of lipoic acid cell factory

BS1912 was constructed by curing the Keio Δ*lipA* strain of its *kanR* marker. MAGE used moBS150, introducing the IscR *C92Y* point mutation into BS1912, as described above, resulting in BS2114. The *lipA* and truncated *aceF* (Ali and Guest, 1990) genes were amplified from genomic *E. coli* DNA with PhusionU polymerase using, respectively, oBS2200 + oBS2197 and oBS2274 + oBS2277. By amplifying pBS0910 with oBS1587 + oBS1591 using PhusionU polymerase, *lipA* was USER-cloned behind the IPTG inducible promoter, T5lacO (Cavaleiro et al., 2015). The resulting plasmid, pBS0992, was amplified with oBS1468 + oBS2273 using PhusionU polymerase and truncated *aceF* was USER-cloned behind a strong constitutive promoter, apFAB309. Cloned plasmids were transformed into homemade RbCl chemically competent BS1912 and BS2114. Plasmids were purified and sequenced verified with Sanger sequencing. BS1912 and BS2114 containing the correctly assembled plasmid, pBS1037, with constitutively expressed, truncated *aceF* and IPTG-inducible *lipA*, were used for lipoic acid production and LipA toxicity experiments.

4.7. Construction of thiamine cell factory

The two native operons involved in thiamine biosynthesis, *thiC* and *thiM*, were amplified from *E. coli* MG1655 genomic DNA using Phusion High-Fidelity Polymerase (Thermo Scientific, F530L) according to the manufacturer's instructions. Primer pairs oGEN227 + oGEN264 and oBS421 + oBS422 were used to introduce 25–33 bp of homology overlap with the target backbones and a strong RBS in front of the first genes of *thiC* and *thiM,* respectively. Two empty backbone plasmids carrying strong apFAB promoters (Vivek K Mutalik et al., 2013) pBS100 (apFAB46) and pGEN50 (apFAB71) were linearized by PCR using Phusion polymerase and oligos oGEN265 and oGEN266. The *thiC*-operon was introduced to pBS100 and *thiM*-operon was introduced to pGEN50 using Gibson Assembly Master Mix (New England Biolabs, E2611L) according to the manufacturer's protocol (Gibson et al., 2009) and transformed into One Shot TOP10 chemically competent cells (ThermoFisher Scientific, C404006) according to the supplier's instructions. Single colonies isolated on LB agar plates containing kanamycin (50 mg/mL) were used to inoculate 4-ml cultures grown in liquid LB + kanamycin (50 mg/L) overnight for retrieval of assembled plasmids using NucleoSpin Plasmid miniprep kits (Machery-Nagel, 740588) according to the manufacturer's protocol, omitting the optional washing step with AW buffer. Resulting plasmids carrying thiamine operons *thiC* and *thiM* were verified by Sanger sequencing (Eurofins Genomics) to ensure correct assembly, and named pBS116 and pBS117, respectively. The entire plasmid carrying the *thiC*-operon (pBS116) was linearized through PCR using Phusion polymerase and primer pair oGEN289 + oGEN290. The *thiM*-operon including the promoter was amplified from pBS117 with primer pairs oGEN182 + oGEN184. The two linearized operons were assembled into a single plasmid (pBS140) using Gibson Assembly Master Mix, transformed into One Shot TOP10 chemically competent cells, isolated with the NucleoSpin Plasmid miniprep kits and sequenced verified. Finally, the complete thiamine-producing plasmid was introduced into the production strain by electroporation as described above.

4.8. Cloning and evaluation of suf- and isc-libraries

Promoter libraries of native *E. coli suf*- and *isc*-operons (without *iscR*) were made. Plasmid backbone was amplified from pBS1055 using oBS2235-oBS2250 and oBS1468 to introduce promoter variants. The *suf*- and *isc*-operons were amplified from genomic *E. coli* DNA using, respectively, primer pairs oBS2259 + oBS2260 and oBS2264 + oBS2265. All PCR used PhusionU polymerase, for subsequent USER cloning (Cavaleiro et al., 2015), at annealing temperature 60 °C and elongation time 7 min. Ligations were transformed into chemically competent BS1011 strains with pBS412, plated on selective mMOPS plates, incubated at 37°C overnight and verified by colony PCR (56°C annealing temperature, 5 min elongation time) and Sanger sequencing using primers oBS666 + oBS955 (*isc*) and oBS666 + oBS1745 (*suf*) and oBS666 (sequencing). The viability of cells with libraries was very low, resulting in only 4 unique constructs based on sequencing of 96 clones: 1 for the *isc*-operon and 3 for the *suf*-operon.

PCR reactions were in total volume 50 μl, with 1.5 μl each primer (10 μM stock; when several primers were used, 1.5 μl of a pre-mixed pool was added), 1 μl template (< 10 ng total), 1 μl polymerase, 10 μl 5x HF buffer, 1.5 μl dNTP (10 mM) and 34.5 μl MilliQ water. For colony PCR, reactions were scaled to 10 μl using X7 polymerase. For USER

cloning, ~1 pmol total fragments in equimolar amounts were used, mixed with 1 μl DpnI enzyme and 1μl DpnI buffer (10x). Reaction volumes were adjusted to 10 μl with MilliQwater and incubated for 15 min at 37°C. To reactions, 1 μl USER enzyme was added for incubation for 15 min at 37°C, followed by 15 min incubation at room temperature.

4.9. Production of biotin, thiamine and lipoic acid

All production tests used a similar protocol. Single colonies were picked for preculturing in 400 μl minimal MOPS with necessary antibiotics (ampicillin, 100 mg/mL; kanamycin 50 mg/mL; spectinomycin, 50 mg/mL; and/or chloramphenicol 30 mg/mL) in deep-well plates (DWPs) sealed with breathable seal and incubated overnight at 37°C with shaking (250 rpm). Precultures were used to inoculate 400 μl production cultures in DWPs to initial OD600 0.01. Production cultures were in minimal MOPS with necessary antibiotics with DTB (0.1 g/L) for biotin production or octanoic acid (0.6 g/L) for lipoic acid production. Production cultures were incubated for 24 h at 37°C with shaking (250 rpm), sealed with breathable seals. For experiments with growth profiles, 600 μl production cultures were prepared. Before incubation, 200 μl was transferred to a microtiter plate, sealed with transparent breathable seal and OD monitored every 20 min using a microplate photometer (Multiskan FC, Thermo Scientific). OD600 of production cultures was measured at the end of incubation, cells were spun at 5000 G for 5 min, and supernatants transferred to detect product.

4.10. Bioassay for biotin detection

We used a modified version of a published liquid bioassay (Demoll and Shive, 1986) using *E. coli* BW25113 Δ*bioB* (BS1011) with ZeoR plasmid pBS451 as the bioassay strain that was unable to grow on any amount of DTB. A single colony from an LB plate with zeocin (40 mg/L) was used to inoculate minimal MOPS media with zeocin (40 mg/L) for growth at 37°C overnight starved for biotin. Bioassay medium was made by diluting the bioassay culture in minimal MOPS medium with zeocin (40 mg/L) to a final OD600 of 0.01. In a microtiter plate, 15 μl sample supernatant was mixed with 135 μl bioassay medium. Separate wells contained a standard curve with known concentrations of biotin in bioassay medium. Plates were sealed with breathable seals and incubated at 37°C for 20 h with shaking 250 rpm. OD600 was measured and biotin concentrations calculated. If necessary, sample supernatants were diluted to be in range of the bioassay.

4.11. Thiochrome assay for thiamine detection

Thiamine and thiamine derivatives (thiamine monophosphate and thiamine pyrophosphate) in the supernatants of production samples were measured by derivatization to fluorescent thiochromes as described (Genee et al., 2016). Briefly, 50 μl supernatant was mixed with 100 μl 4 M potassium acetate in black microtiter plates and 50 μl freshly prepared 3.8 M potassium ferricyanide in 7 M NaOH was added and mixed by pipetting. Quenching was by adding 50 μl fresh 0.06% H_2O_2 in saturated KH_2PO_4. Fluorescence emission was measured at 444 nm after excitation at 365 nm and concentration of thiamines estimated based on comparison to standard curves included in the derivatization plate.

4.12. Bioassay for lipoic acid detection

An assay similar to our biotin bioassay was set up based on the *E. coli* BW25113 Δ*lipA* strain (BS1912) with a ZeoR plasmid (pBS451) as the bioassay strain. Liquid bioassays were based on a previous publication (Herbert and Guest, 1970). A single colony of the bioassay strain from an LB plate with zeocin (40 mg/L) was used to inoculate minimal MOPS succinate media with zeocin (50 mg/L) for growth at 37°C overnight, starved for lipoic acid. Usually no detectable growth was observed, and cultures were used directly as bioassay medium. In microtiter plates, 15 μl sample supernatant was mixed with 135 μl bioassay medium. A standard curve with known concentrations of lipoic acid in bioassay medium was included in separate wells. Plates were sealed with breathable seal and incubated at 37°C for 20 h with shaking at 250 rpm before measuring OD600 and calculating lipoic acid concentrations. Sample supernatants were diluted if necessary, to be in range of the bioassay.

4.13. Proteomics analysis

Label-free proteomics was carried out at Groningen University by the Molecular Systems Biology group led by Professor Matthias Heinemann as described (Schmidt et al., 2015). Precultures were inoculated with single colonies in mMOPS media with ampicillin (100 μg/mL) and incubated at 37°C with 250 rpm shaking overnight before using to inoculate 50 mL mMOPS with ampicillin and either 0.025 mM IPTG or 1 mM IPTG in a 250 mL baffled shaker flask to initial OD600 0.001. Flasks were incubated at 37°C with 250 rpm shaking for 10 generations (OD600–0.5) and 8×10^8 cells were harvested in technical triplicates by centrifuging at 4°C at 17,000 G for 3 min. Supernatants were evaluated for production using bioassays and cell pellets were washed twice in 2 mL icecold PBS buffer. Cell pellets were snap-frozen in liquid nitrogen and stored at −80°C until mass spectrometry (MS)-MS-analysis.

Data were normalized as the percentage fraction of each protein to the total amount of protein in each sample, based on intensity-based quantification (iBAQ) values for each strain as

$$\textit{Protein fraction}\ (\%) = \frac{iBAQ\ [specific\ protein]}{iBAQ\ [total\ protein]} \cdot 100$$

Data were analyzed based on ANOVA multiple comparison test with 95% confidence intervals applying Bonferroni-correction using the MaxQuant software Perseus (Tyanova et al., 2016). Prior to analysis, data with a quality score (measure of false discovery rate) of more than 0.01 were removed, together with proteins undetected in more than 30% of the samples.

4.14. Calculations of productivities for biotin cell factories reported in literature

Productivities were calculated for end-point measurements reported for *B. subtilis* (Van Arsdell et al., 2005), *P. mutabilis* (Xiao et al., 2019), and *S. marcescens* (Masuda et al., 1995), using conversion factors for OD600 to g cell dry weight (gCDW) reported in literature of 0.322 for *B. subtilis* (Wenzel et al., 2011) and of 0.4 for *E. coli* (Glazyrina et al., 2010). As no value was reported for *P. mutabilis*, it is assumed to be similar to *P. putida* of 0.4 (Azoddein et al., 2017).

Author contributions

A.P.B., H.J.G., and **L.S.G.** conceptualization with input from **M.O.A.S**. **A.P.B., D.L.H.**, and **N.M.P.**:Methodology and Validation. **A.P.B., D.L.H., J.B.,** and **B.S.**: Resources. **A.P.B.** and **D.L.H**: Investigation. **A.P.B.:** Writing – Original Draft, Review and Editing, with inputs from all authors.

Declaration of competing interest

Biosyntia ApS has filed a patent application based on the results of this paper.

Acknowledgements

We thank Johan Hekelaar (Molecular Systems Biology, Groningen University, The Netherlands) for performing proteomics. We further thank Gijs Verkleij for assistance with MAGE of combinatorial IscR mutants. A.P.B acknowledges funding from Innovation Foundation Denmark (Industrial Ph.D. program, No. 5016-00135B). L.S.G and H.J.G acknowledge funding from the European Union's Horizon 2020 research and innovation programme under grant agreement no. 686070, DD-DeCaf. M.O.A.S. acknowledges funding from The Novo Nordisk Foundation under NFF grant number: NNF10CC1016517.

Appendix A. Supplementary data

Supplementary data to this article can be found online at https://doi.org/10.1016/j.ymben.2020.03.005.

References

Reyda, M.R., Dippold, R., Dotson, M.E., Jarrett, J.T., 2008. Loss of iron sulfur clusters from biotin synthase as a result of catalysis promotes unfolding and degradation. Arch. Biochem. Biophys. 471, 32–41. https://doi.org/10.1016/j.mib.2008.09.004. Bacteriophage.

Acevedo-Rocha, C.G., Gronenberg, L.S., Mack, M., Commichau, F.M., Genee, H.J., 2019. Microbial cell factories for the sustainable manufacturing of B vitamins. Curr. Opin. Biotechnol. 56, 18–29. https://doi.org/10.1016/j.copbio.2018.07.006.

Akhtar, M.K., Jones, P.R., 2008. Deletion of iscR stimulates recombinant clostridial Fe-Fe hydrogenase activity and H2-accumulation in Escherichia coli BL21(DE3). Appl. Microbiol. Biotechnol. 78, 853–862. https://doi.org/10.1007/s00253-008-1377-6.

Ali, S.T., Guest, J.R., 1990. Isolation and characterization of lipoylated and unlipoylated domains of the E2p subunit of the pyruvate dehydrogenase complex of Escherichia coli. Biochem. J. 271, 139–145.

Azoddein, A.A.M., Ahmad, M.M., Yunus, R.M., Sulaiman, N.M.N., 2017. Effect of acclimatization time to microbial cell growth and biosynthesis of mesophilic gamma-proteobacterium, in orbital shake flasks. MATEC Web Conf 109. https://doi.org/10.1051/matecconf/201710904003.

Berkovitch, F., Nicolet, Y., Wan, J.T., Jarrett, J.T., Drennan, C.L., 2004. Crystal structure of biotin synthase, an S-adenosylmethionine-dependent radical enzyme. Science 303, 76–79. https://doi.org/10.1126/science.1088493. (80-.).

Bitoun, J.P., Wu, G., Ding, H., 2008. Escherichia coli FtnA acts as an iron buffer for re-assembly of iron-sulfur clusters in response to hydrogen peroxide stress. Biometals 21, 693–703. https://doi.org/10.1007/s10534-008-9154-7.

Bonde, M.T., Klausen, M.S., Anderson, M.V., Wallin, A.I.N., Wang, H.H., Sommer, M.O.A., 2014. MODEST: a web-based design tool for oligonucleotide-mediated genome engineering and recombineering. Nucleic Acids Res. 42, 408–415. https://doi.org/10.1093/nar/gku428.

Broderick, J.B., Duffus, B.R., Duschene, K.S., Shepard, E.M., 2014. Radical S-adenosylmethionine enzymes. Chem. Rev. 114, 4229–4317. https://doi.org/10.1021/cr4004709.

Brown, S.W., Komagowa, K., 1991. The production of biotin by genetically modified micro-organisms. Biotechnol. Genet. Eng. Rev. 9, 295–326.

Brown, S.W., Speck, D., Sabatié, J., Gloeckler, R., O'Regan, M., Viret, J.F., Lemoine, Y., Ohsawa, I., Kisou, T., Hayakawa, K., Kamogawa, K., 1991. The production of biotin by recombinant strains of Escherichia coli. J. Chem. Technol. Biotechnol. 50, 115–121. https://doi.org/10.1002/jctb.280500114.

Cardinale, S., Tueros, F.G., Sommer, M.O.A., 2017. Genetic-metabolic coupling for targeted metabolic engineering. Cell Rep. 20, 1029–1037. https://doi.org/10.1016/j.celrep.2017.07.015.

Cavaleiro, A.M., Kim, S.H., Seppälä, S., Nielsen, M.T., Nørholm, M.H.H., 2015. Accurate DNA assembly and genome engineering with optimized uracil excision cloning. ACS Synth. Biol. 4, 1042–1046. https://doi.org/10.1021/acssynbio.5b00113.

Choi-Rhee, E., Cronan, J.E., 2005. A nucleosidase required for in vivo function of the S-adenosyl-L-methionine radical enzyme, biotin synthase. Chem. Biol. 12, 589–593. https://doi.org/10.1016/j.chembiol.2005.04.012.

Cramer, J.D., Jarrett, J.T., 2018. Purification, characterization, and biochemical assays of biotin synthase from Escherichia coli. In: Methods in Enzymology, first ed. Elsevier Inc. https://doi.org/10.1016/bs.mie.2018.06.003.

Cronan, J.E., 2013. Biotin and lipoic acid: synthesis, attachment, and regulation. EcoSal Plus 1, 217–244. https://doi.org/10.1128/ecosalplus.ESP-0001-2012.

Cronan, J.E., 2014. Biotin and lipoic acid: synthesis, attachment and regulation. EcoSal Plus 18, 1199–1216. https://doi.org/10.1128/ecosalplus.ESP-0001-2012.Biotin.

Cronan, J.E., Zhao, X., Jiang, Y., 2005. Function, Attachment and Synthesis of Lipoic Acid in Escherichia coli, Advances in Microbial Physiology. Elsevier Masson SAShttps://doi.org/10.1016/S0065-2911(05)50003-1.

Delano, W.L., 2002. The PyMOL Molecular Graphics System. DeLano Sci. LLC, San Carlos, CA.

Demoll, E., Shive, W., 1986. Assay for biotin in the presence of dethiobiotin with lactobacillus plantarum. Anal. Biochem. 158, 55–58.

Eggersdorfer, M., Laudert, D., Létinois, U., McClymont, T., Medlock, J., Netscher, T., Bonrath, W., 2012. One hundred years of vitamins-a success story of the natural sciences. Angew. Chem., Int. Ed. Engl. 51, 12960–12990. https://doi.org/10.1002/anie.201205886.

Ezraty, B., Gennaris, A., Barras, F., Collet, J.-F., 2017. Oxidative stress, protein damage and repair in bacteria. Nat. Rev. Microbiol. 15, 385–396. https://doi.org/10.1038/nrmicro.2017.26.

Ferla, M.P., Patrick Correspondence, W.M., Patrick, W.M., 2019. Bacterial Methionine Biosynthesis. https://doi.org/10.1099/mic.0.077826-0.

Fleischhacker, A.S., Stubna, A., Hsueh, K.L., Guo, Y., Teter, S.J., Rose, J.C., Brunold, T.C., Markley, J.L., Münck, E., Kiley, P.J., 2012. Characterization of the [2Fe-2S] cluster of Escherichia coli transcription factor IscR. Biochemistry 51, 4453–4462. https://doi.org/10.1021/bi3003204.

Genee, H.J., Bali, A.P., Petersen, S.D., Siedler, S., Bonde, M.T., Gronenberg, L.S., Kristensen, M., Harrison, S.J., Sommer, M.O.A., 2016. Functional mining of transporters using synthetic selections. Nat. Chem. Biol. 12, 1015–1022. https://doi.org/10.1038/nchembio.2189.

Gibson, D.G., Young, L., Chuang, R.-Y., Venter, J.C., Hutchison, C. a, Smith, H.O., 2009. Enzymatic assembly of DNA molecules up to several hundred kilobases. Nat. Methods 6, 343–345. https://doi.org/10.1038/nmeth.1318.

Giel, J.L., Rodionov, D., Liu, M., Blattner, F.R., Kiley, P.J., 2006. IscR-dependent gene expression links iron-sulphur cluster assembly to the control of O2-regulated genes in Escherichia coli. Mol. Microbiol. 60, 1058–1075. https://doi.org/10.1111/j.1365-2958.2006.05160.x.

Glazyrina, J., Materne, E.M., Dreher, T., Storm, D., Junne, S., Adams, T., Greller, G., Neubauer, P., 2010. High cell density cultivation and recombinant protein production with Escherichia coli in a rocking-motion-type bioreactor. Microb. Cell Factories 9, 1–11. https://doi.org/10.1186/1475-2859-9-42.

Gräwert, T., Kaiser, J., Zepeck, F., Laupitz, R., Hecht, S., Amslinger, S., Schramek, N., Schleicher, E., Weber, S., Haslbeck, M., Buchner, J., Rieder, C., Arigoni, D., Bacher, A., Eisenreich, W., Rohdich, F., 2007. IspH protein of Escherichia c oli : studies on Iron − Sulfur cluster implementation and catalysis. J. Am. Chem. Soc. 126, 12847–12855. https://doi.org/10.1021/ja0471727.

Herbert, A.A., Guest, J.R., 1970. Turbidimetric and polarographic assays for lipoic acid using mutants of Escherichia coli. Methods Enzymol. 18, 269–272. https://doi.org/10.1016/0076-6879(71)18314-0.

Ifuku, O., Koga, N., Haze, S., Kishimoto, J., Arai, T., Wachi, Y., 1995. Molecular analysis of growth inhibition caused by overexpression of the biotin operon in Escherichia coli. Biosci. Biotechnol. Biochem. 59, 184–189. https://doi.org/10.1080/bbb.59.184.

Imlay, J.A., 2006. Iron-sulphur clusters and the problem with oxygen. Mol. Microbiol. 59, 1073–1082. https://doi.org/10.1111/j.1365-2958.2006.05028.x.

Jarrett, J.T., 2005. Biotin synthase: enzyme or reactant? Chem. Biol. 12, 409–410. https://doi.org/10.1016/j.chembiol.2005.04.003.

Jurgenson, C.T., Begley, T.P., Ealick, S.E., 2009. The structural and biochemical foundations of thiamin biosynthesis. Annurev. Biochem. 78, 569–603. https://doi.org/10.1146/annurev.biochem.78.072407.102340.

Kanai, T., Takahashi, K., Inoue, H., 2006. Three distinct-type glutathione S-transferases from Escherichia coli important for defense against oxidative stress. J. Biochem. 140, 703–711. https://doi.org/10.1093/jb/mvj199.

Kriek, M., Peters, L., Takahashi, Y., Roach, P.L., 2003. Effect of iron-sulfur cluster assembly proteins on the expression of Escherichia coli lipoic acid synthase. Protein Expr. Purif. 28, 241–245. https://doi.org/10.1016/S1046-5928(02)00680-0.

Kuchenreuther, J.M., Grady-Smith, C.S., Bingham, A.S., George, S.J., Cramer, S.P., Swartz, J.R., 2010. High-yield expression of heterologous [FeFe] hydrogenases in Escherichia coli. PloS One 5, e15491. https://doi.org/10.1371/journal.pone.0015491.

Li, X.-X., Liu, Q., Liu, X.-M., Shi, H.-W., Chen, S.-F., 2016. Using synthetic biology to increase nitrogenase activity. Microb. Cell Factories 15, 43. https://doi.org/10.1186/s12934-016-0442-6.

Masuda, M., Takahashi, S., Sakurai, N., Yanagiya, K., Komatsubara, S., Tosa, T., 1995. Further improvement of D-biotin production by a recombinant strain of Serratia marcescens. Process Biochem. 30, 553–562. https://doi.org/10.1016/0032-9592(94)00060-U.

McCarthy, E.L., Booker, S.J., 2017. Destruction and reformation of an iron-sulfur cluster during catalysis by lipoyl synthase. Science 358, 373–377. https://doi.org/10.1126/science.aan4574. (80-.).

Nahlik, M.S., Brickman, T.J., Ozenberger, B.A., McIntosh, M.A., 1989. Nucleotide sequence and transcriptional organization of the Escherichia coli enterobactin biosynthesis cistrons entB and entA. J. Bacteriol. 171, 784–790. https://doi.org/10.1128/jb.171.2.784-790.1989.

Nakamura, M., Saeki, K., Takahashi, Y., 1999. Hyperproduction of recombinant ferredoxins in *Escherichia coli* by coexpression of the ORF1-ORF2-*iscS-iscU-iscA-hscB-hs cA-fdx*-ORF3 gene cluster. J. Biochem. 126, 10–18. https://doi.org/10.1093/oxfordjournals.jbchem.a022409.

Palmer, L.D., Downs, D.M., 2013. The thiamine biosynthetic enzyme ThiC catalyzes multiple turnovers and is inhibited by S-adenosylmethionine (AdoMet) metabolites. J. Biol. Chem. 288, 30693–30699. https://doi.org/10.1074/jbc.M113.500280.

Parveen, N., Cornell, K. a, 2011. Methylthioadenosine/S-adenosylhomocysteine nucleosidase, a critical enzyme for bacterial metabolism. Mol. Microbiol. 79, 7–20. https://doi.org/10.1111/j.1365-2958.2010.07455.x.

Price, C.E., Driessen, A.J.M., 2010. Biogenesis of membrane bound respiratory complexes in Escherichia coli. Biochim. Biophys. Acta Mol. Cell Res. 1803, 748–766. https://doi.org/10.1016/j.bbamcr.2010.01.019.

Py, B., Barras, F., 2010. Building Fe–S proteins: bacterial strategies. Nat. Rev. Microbiol. 8, 436–446. https://doi.org/10.1038/nrmicro2356.

Qiu, X., Zhang, H., Yin, Y., Brandes, H., Marsala, T., Stenerson, K., Cramer, H., 2019. Determination of active vitamin B12 (cobalamin) in dietary supplements and ingredients by reversed-phase liquid chromatography: single-laboratory validation.

Food Chem. 12, 125010. https://doi.org/10.1016/j.foodchem.2019.125010.
Rajagopalan, S., Teter, S.J., Zwart, P.H., Brennan, R.G., Phillips, K.J., Kiley, P.J., 2013. Studies of IscR reveal a unique mechanism for metal-dependent regulation of DNA binding specificity. Nat. Struct. Mol. Biol. 20, 740–747. https://doi.org/10.1038/nsmb.2568.
Rugbjerg, P., Sommer, M.O.A., 2019. Overcoming genetic heterogeneity in industrial fermentations. Nat. Biotechnol. 37, 869–876. https://doi.org/10.1038/s41587-019-0171-6.
Rugbjerg, P., Myling-Petersen, N., Porse, A., Sommer, M., 2018. Diverse genetic error modes constrain large-scale bio-based production. Nat. Commun. 9, 787. https://doi.org/10.1038/s41467-018-03232-w.
Sakurai, N., Imai, Y., Masuda, M., Komatsubara, S., Tosa, T., 1993. Construction of a biotin-overproducing strain of Serratia marcescens. Appl. Environ. Microbiol. 59, 2857–2863.
Sakurai, N., Imai, Y., Komatsubara, S., 1995. Instability of the mutated biotin operon plasmid in a biotin-producing mutant of Serratia marcescens. J. Biotechnol. 43, 11–19. https://doi.org/10.1016/0168-1656(95)00103-9.
Salis, H.M., 2011. The ribosome binding site calculator. Methods Enzymol. 498, 19–42. https://doi.org/10.1016/B978-0-12-385120-8.00002-4.
Schmidt, A., Kochanowski, K., Vedelaar, S., Ahrne, E., Volkmer, B., Callipo, L., Knoops, K., Bauer, M., Aebersold, R., Heinemann, M., 2015. The quantitative and condition-dependent Escherichia coli proteome. Nat. Biotechnol. 34, 104–110. https://doi.org/10.1038/nbt.3418.
Schwechheimer, S.K., Park, E.Y., Revuelta, J.L., Becker, J., Wittmann, C., 2016. Biotechnology of riboflavin. Appl. Microbiol. Biotechnol. 100, 2107–2119. https://doi.org/10.1007/s00253-015-7256-z.
Schyns, G., Geng, Y., Barbosa, T.M., Henriques, A., Perkins, J.B., 2005. Isolation and characterization of new thiamine-deregulated mutants of Bacillus subtilis. J. Bacteriol. 187, 8127–8136. https://doi.org/10.1128/JB.187.23.8127.
Streit, W.R., Entcheva, P., 2003. Biotin in microbes, the genes involved in its biosynthesis, its biochemical role and perspectives for biotechnological production. Appl. Microbiol. Biotechnol. 61, 21–31. https://doi.org/10.1007/s00253-002-1186-2.
Sun, Y., Zhang, W., Ma, J., Pang, H., Wang, H., 2017. Overproduction of α-lipoic acid by gene manipulated Escherichia coli. PloS One 12, e0169369. https://doi.org/10.1371/journal.pone.0169369.
Tyanova, S., Temu, T., Sinitcyn, P., Carlson, A., Hein, M.Y., Geiger, T., Mann, M., Cox, J., 2016. The Perseus computational platform for comprehensive analysis of (prote) omics data. Nat. Methods 13, 731–740. https://doi.org/10.1038/nmeth.3901.
Mutalik, V.K., Guimaraes, J.C., Cambray, G., Mai, Q.A., Christoffersen, M.J., Martin, L., Yu, A., Lam, C., Rodriguez, C., Bennett, G., Keasling, J.D., Endy, D., Arkin, A.P., 2013. Quantitative estimation of activity and quality for collections of functional genetic elements. Nat. Methods 10, 347–353. https://doi.org/10.1038/nmeth.2403.
Van Arsdell, S.W., Perkins, J.B., Yocum, R.R., Luan, L., Howitt, C.L., Chatterjee, N.P., Pero, J.G., 2005. Removing a bottleneck in the Bacillus subtilis biotin pathway: bioA utilizes lysine rather than S-adenosylmethionine as the amino donor in the KAPA-to-DAPA reaction. Biotechnol. Bioeng. 91, 75–83. https://doi.org/10.1002/bit.20488.
Mutalik, Vivek K., Guimaraes, J.C., Cambray, G., Lam, C., Christoffersen, M.J., Mai, Q.-A., Tran, A.B., Paull, M., Keasling, J.D., Arkin, A.P., Endy, D., 2013. Precise and reliable gene expression via standard transcription and translation initiation elements. Nat. Methods 10, 354–360. https://doi.org/10.1038/nmeth.2404.
Wang, H.H., Church, G.M., 2011. Multiplexed genome engineering and genotyping methods: applications for synthetic biology and metabolic engineering. In: Methods in Enzymology, first ed. Elsevier Inc. https://doi.org/10.1016/B978-0-12-385120-8.00018-8.
Wenzel, M., Müller, A., Siemann-Herzberg, M., Altenbuchner, J., 2011. Self-inducible Bacillus subtilis expression system for reliable and inexpensive protein production by high-cell-density fermentation. Appl. Environ. Microbiol. 77, 6419–6425. https://doi.org/10.1128/AEM.05219-11.
Xiao, F., Wang, H., Shi, Z., Huang, Q., Huang, L., Lian, J., Cai, J., Xu, Z., 2019. Multi-level metabolic engineering of Pseudomonas mutabilis ATCC31014 for efficient production of biotin. Metab. Eng. (April), 1–10. https://doi.org/10.1016/j.ymben.2019.05.005.
Yang, L., Mih, N., Anand, A., Park, J.H., Tan, J., Yurkovich, J.T., Monk, J.M., Lloyd, C.J., Sandberg, T.E., Seo, S.W., Kim, D., Sastry, A.V., Phaneuf, P., Gao, Y., Broddrick, J.T., Chen, K., Heckmann, D., Szubin, R., Hefner, Y., Feist, A.M., Palsson, B.O., 2019. Cellular responses to reactive oxygen species can be predicted on multiple biological scales from molecular mechanisms. Proc. Natl. Acad. Sci. 201905039. https://doi.org/10.1073/pnas.1905039116.
Yeo, W.S., Lee, J.H., Lee, K.C., Roe, J.H., 2006. IscR acts as an activator in response to oxidative stress for the suf operon encoding Fe-S assembly proteins. Mol. Microbiol. 61, 206–218. https://doi.org/10.1111/j.1365-2958.2006.05220.x.
Zhang, Z., Feige, J.N., Chang, A.B., Anderson, I.J., Brodianski, V.M., Vitreschak, A.G., Gelfand, M.S., Saier, M.H., 2003. A transporter of Escherichia coli specific for L- and D-methionine is the prototype for a new family within the ABC superfamily. Arch. Microbiol. 180, 88–100. https://doi.org/10.1007/s00203-003-0561-4.